

NUMERICAL PREDICTION OF GTD-350 TURBOSHAFT ENGINE COMBUSTOR DETERIORATION

Maciej Chmielewski

*Institute of Aviation
Krakowska Avenue 110/114, 02-256 Warsaw, Poland
tel.: +48228460011, fax: +48228464432, e-mail: maciej.chmielewski@ilot.edu.pl*

Szymon Fulara, Marian Gieras

*Warsaw University of Technology
Institute of Heat Engineering
Nowowiejska Street 21/25, 00-665 Warsaw, Poland
tel.: +48 22 2345222
e-mail: szymon.fulara@itc.pw.edu.pl*

Abstract

The aim of this article is to describe the use of Computational Fluid Dynamics (CFD) model for turboshaft combustor chamber deterioration analysis. To show advantages of the proposed approach the test bench of GTD-350 turboshaft engine operating at the Institute of Heat Engineering, Warsaw University of Technology was used as an example. The CFD modelling of the reactive flow inside 40° sector of GTD-350 engine section was developed. Proposed modelling technique provides good correlations with experimental data and shows that the combustor front wall soot accumulation is clearly related to the fuel droplets residence time and the oxygen mass fraction. The temperature distribution inside the combustion chamber allows concluding on possible hot distress areas on the combustion chamber liner walls. Engine borescope inspection (BSI) of the compressor, combustion chamber, compressor turbine and power turbine is used to correlate model predictions with a real GTD-350 engine deterioration. Very good correlation of the engine BSI observations with the numerical predictions proves usefulness of the developed model. Finally, advantages and future applications of the developed model are discussed.

Keywords: turboshaft engine, engine health monitoring, digital analytics, engine deterioration, CFD modelling

1. Introduction

Strict safety regulations and rapid progress in the design of turbine engines made them the most reliable machines nowadays. The overhaul of the turbine engines has become one of the most profitable businesses; therefore, the key factor of success in aviation industry is competent costs management [1-3]. Standard procedure to replace elements and parts based on time of operation is not optimal. Either the relatively good and durable elements are replaced or actual condition has to be assessed during extensive and time-consuming inspections. One of the very promising ideas related to data collected by devices is digital engine analytics.

Currently, statistical based analytical models are the most frequently used methods for Engine Health Monitoring. Artificial neural networks, support vector machines (SVM) and particle swarm optimization (PSO) techniques are also utilized in order to improve the accuracy of the predictions [4-7]. It has been proven that a hybrid PSO-SVM-based model can give a regression accuracy of about 95% [8]. It is worth noting that described methods can be used only when historical data from the large engine population is available. For new engines, where no or very limited data is available statistical methods do not provide satisfying accuracy.

In general, it can be concluded that the physical models based on the full or partial flight parameters provide the most accurate results [9, 10]. In this article, authors propose the use of the Computational Fluid Dynamics (CFD) model for turboshaft combustor chamber deterioration analysis. The developed model is compared with the real GTD-350 combustion chamber condition obtained by means of engine borescope inspection.

In the final part of the article, the advantages of the proposed model and model accuracy are discussed. Lastly, possible physical applications of the model are presented.

2. Engine and test bench

The object of the study presented in this article is GTD-350 turboshaft engine (after overhaul life and several years of working on a test bench) located at engine test bench at the Institute of Heat Engineering, Warsaw University of Technology (Fig. 1). GTD-350 turboshaft engine serves as a propulsion system for Mi-2 helicopter. The initial design is based on American Allison 250 turbine engine and has been developed by Klimov Experimental Design Bureau. In 1966 thanks to SSSR-Polish agreement the production of both, engine and helicopter, has been moved to PZL Świdnik Aviation Company [11]. Between 1966 and 2005 over 5000 Mi-2s with over 11,000 engines have been manufactured and delivered to various customers around the world.



Fig. 1. GTD-350 digital test bench at the Institute of Heat Engineering, Warsaw University of Technology

GTD-350 engine consists of seven axial and one centrifugal compressor stages; single, cylindrical reversed flow combustion chamber; single stage compressor turbine and two stages power turbine. Engine is controlled by ST-1 hydro-pneumatic unit, with centrifugal power turbine speed limiter, OOWT-3. The combustor Exhaust Gas Temperature (EGT) is measured using WUTT200 thermocouples. Ignition plug is a solid-state semiconductor, SP-1SU. Starting control system contains a transmitter with programming mechanism (PSG-14A). Engine is also equipped with air bleed valves allowing automatic air to atmosphere release to avoid compressor stall and anti-icing system. Digital engine test stand has also been equipped with controllers monitoring main engine parameters: static and total pressure at compressor inlet, total pressure and temperature at the compressor and the combustion chamber outlets and rotational speed sensor. GTD-350 engine produces 235 kW of nominal power and 313 kW of starting power with max. of 45,000 rpm, compressor rotational speed and 24,000 rpm power turbine rotational speed.

Engine test bench of unique capabilities has been built at Warsaw University of Technology. It links analogue, hydro mechanically controlled turboshaft engine with digital panel enabling engine control and data acquisition. Unlike a standard commercial test bench, WUT's digital test bench enables to conduct experiments. Engine test stand scheme is shown in Fig. 2. Engine is controlled by using eddy current brake. Three different control strategies are available for an engine operator:

- supervising the power turbine rotational speed by a controller,
- monitoring and setting the output shaft torque,
- linear way of controlling the engine torque as function of throttle opening,
- an experimental way allowing the independent torque and rotational speed control.

The following multiple engine parameters are measured and registered by numerical data acquisition system:

- rotational speed of the driving shaft (power turbine),
- output torque (or braking torque),
- rotational speed of the HP shaft (turbine and compressor),
- rotational speed of the power turbine,
- exhaust gas temperature at combustion chamber outlet allowing to monitor turbine inlet temperature.

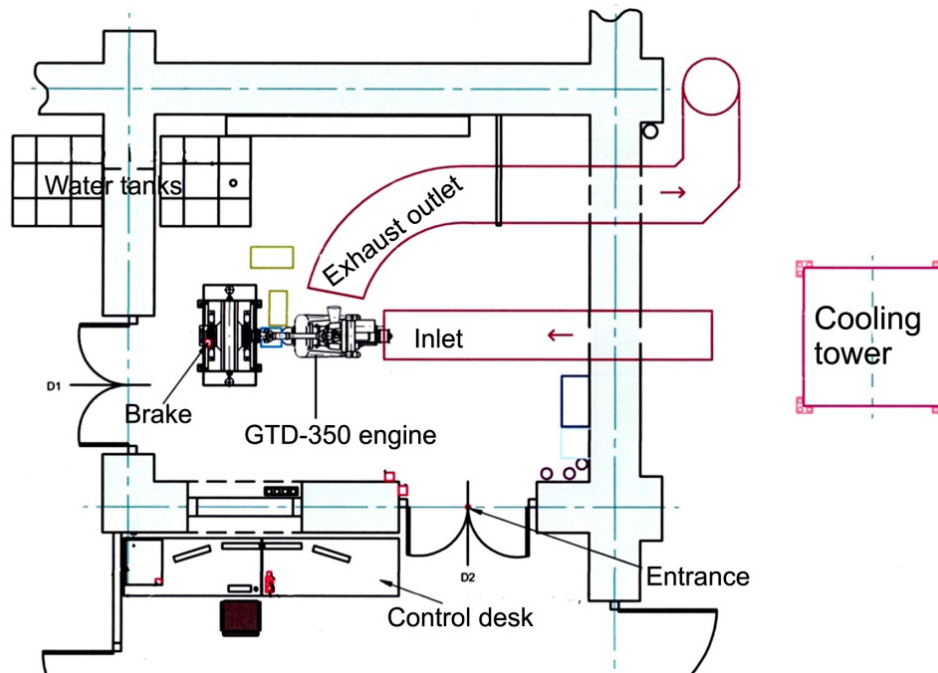


Fig. 2. GTD-350 test bench scheme

3. Numerical simulations

In order to predict the combustor deterioration, a physics based numerical model has been developed. Reactive flow field solution with the use of ANSYS FLUENT v.12.0 Computational Fluid Dynamics (CFD) commercial code has been achieved. Based on the results of the numerical calculations presented in the articles [13-15] (to shorten the time of calculations) a 40° section of the combustor has been selected and meshed with hexahedral elements (Fig. 3). Cyclic symmetry boundary condition has been applied to section sidewalls.

Pressure based, steady state solver has also been used. Since there is highly turbulent flow inside engine combustor, Reynold's Stress Models (RSM), also known as Reynold's Stress Transport (RST) turbulence model has been utilized. This model uses an isotropic eddy viscosity,

solves all components of the turbulent transport, and works well for wide range of engineering flows. Standard wall function has been applied with turbulence model for improved near-wall flow solution. Liquid kerosene has been used as a fuel. Lagrangian Discrete Phase Model (DPM) has been used for fuel injection modelling. Fuel nozzle radius of 0.9 mm with a total mass flow of 0.0045 kg/s (per 40° section) has been used based on fuel nozzle technical data and measurements. Injection velocity has been calculated based on the formula (1).

$$V = \frac{\dot{m}}{\rho A} = \frac{0.040534[\text{kg/s}]}{780[\text{kg/m}^3] \cdot 2.5434 \cdot 10^{-6} [\text{m}^{-2}]} = 20.43 [\text{m/s}]. \quad (1)$$

Mean droplet diameter of $2.5 \cdot 10^{-5}$ m has been assumed based on technical data. Air mass flow supplied from compressor for the assumed engine working parameters equals to $Q_c = 0.243$ [kg/s] (per 40° section).

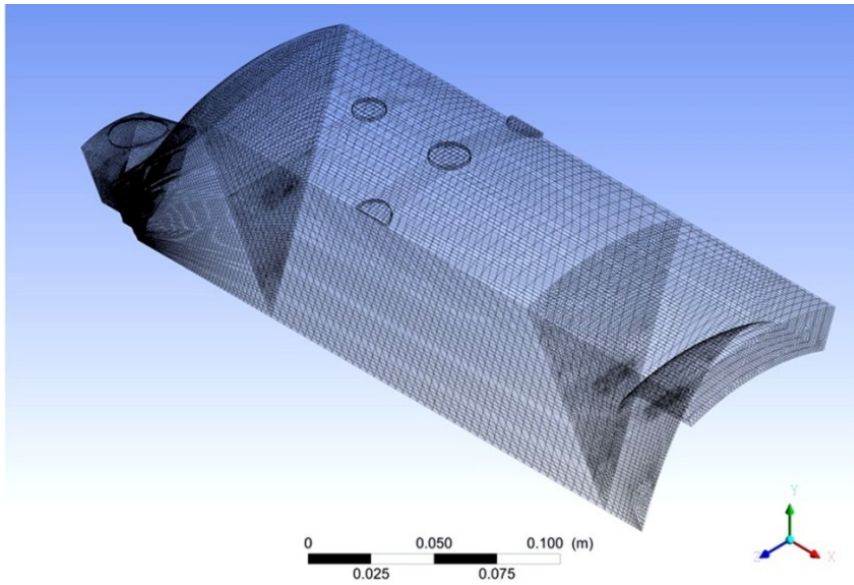


Fig. 3. Computational grid with hexahedral elements

Streamlines and particle residence time are shown in Fig. 4 and 5, respectively. Both parameters were obtained by CFD solution of the flow field inside 40° sector of the combustor.

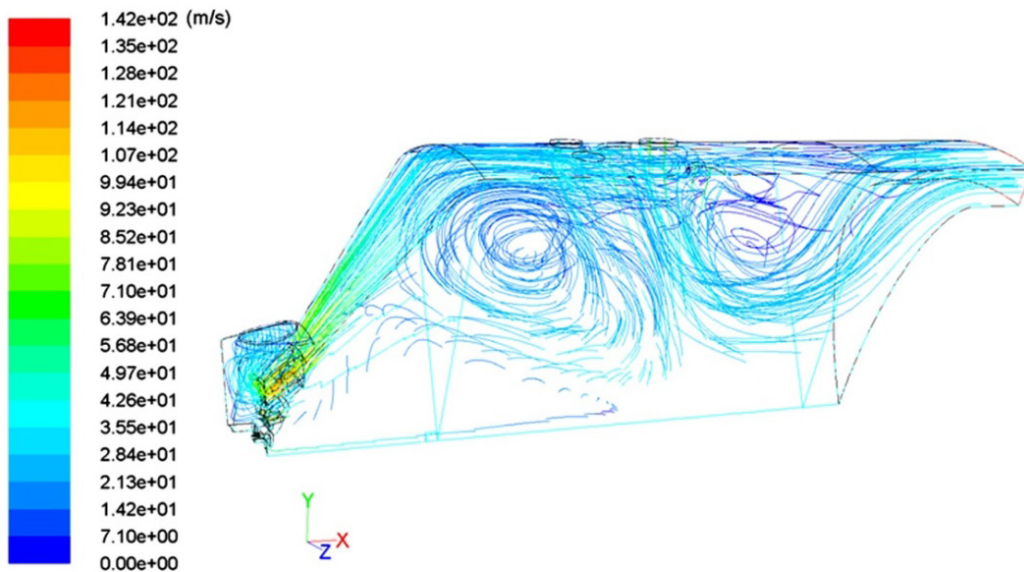


Fig. 4. Streamlines coloured by the velocity

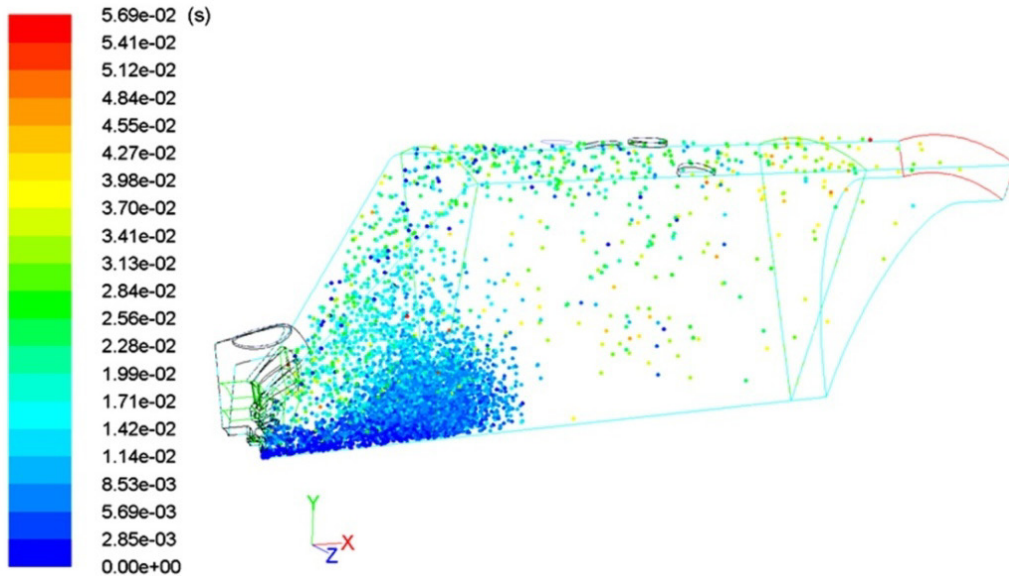


Fig. 5. Droplets distribution coloured by residence time

Combustion is modelled using a *Non-Premixed Combustion* model with fuel and oxidizer entering the reaction zone in distinct streams. The non-premixed combustion model uses a modelling approach that solves transport equations of the mixture fraction. Main chemical species, including radicals and intermediate concentrations are derived from the predicted mixture fraction distribution. Property data for the species are accessed through a chemical database and turbulence-chemistry interaction is modelled using a β -function for the Probability Density Function (PDF) [16]. Discrete ordinates radiation model has been used. Obtained temperature contours are presented in Fig. 6. In Fig. 7, one can see oxygen mass fraction contour plot. Both contour plots are presented on a central section plane.

Maximum noted temperature of 2200 K is located, as one might expect, in the region of the recirculation vortex area (primary combustion zone). Average area-weighted temperature at combustor outlet obtained with numerical modelling equals to 1297 K, which is just 54 K above average combustor outlet temperature from experimental data. Very good correlation between numerical and experimental data was proven despite simplified numerical models.

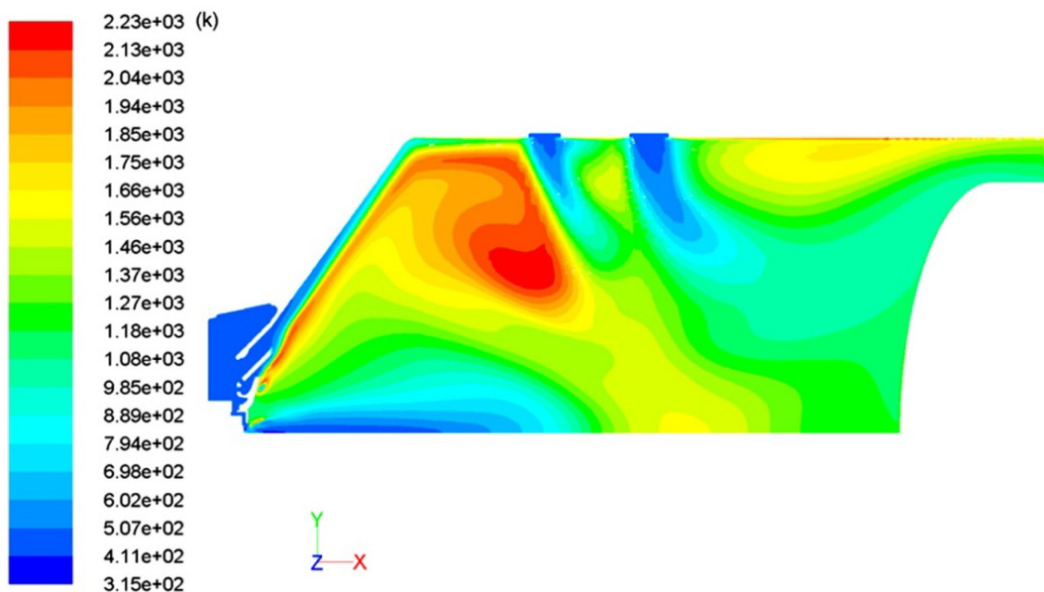


Fig. 6. Temperature contour plot

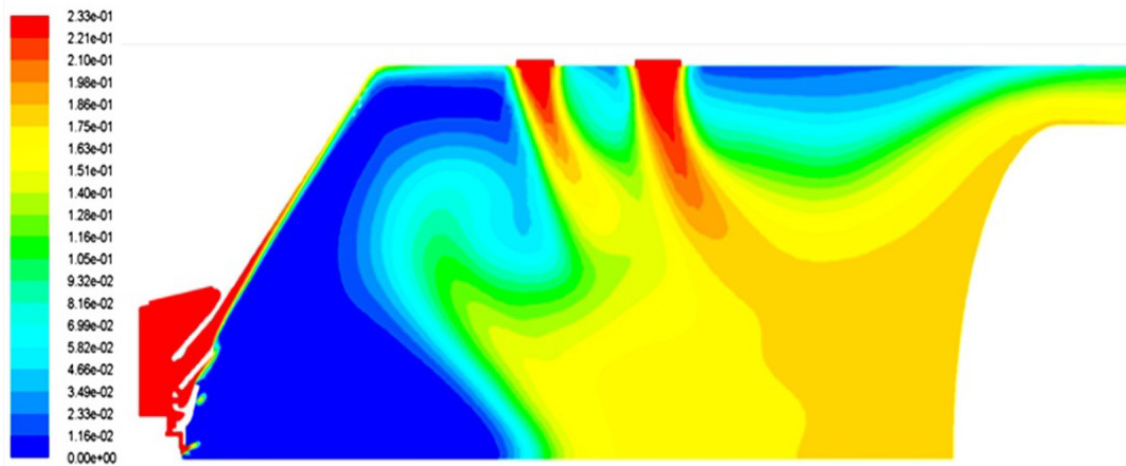


Fig. 7. Oxygen mass fraction contour plot

It is worth noticing that moderately high temperatures are located close to front wall of the combustor chamber. Significant concentration of the fuel droplets (Fig. 5) and low oxygen concentration (fig. 7) together with elevated temperatures may result in incomplete combustion and coking, as a result of fuel dehydrogenation. In order to prevent the soot accumulation, primary swirler modification, optimization of the air distribution and fuel injection should be carried out. Higher swirl number and larger swirler effective area can lead to both: decreased temperatures and better fuel-air mixing process preventing soot accumulation. Changes in the fuel nozzle (i.e. additional fuel circuits, internal air swirler) together with higher injection pressures can prevent coking as well.

4. Engine Borescope Inspection

In order to correlate the conclusions from the numerical model investigation with an actual combustor condition, a borescope inspection of the combustor chamber was conducted. In addition to the combustor, also compressor, compressor turbine nozzles and blades as well as power turbine blades were inspected. Inspection has been performed using HAZET borescope with probe (diameter 4.9 mm) looking laterally – 90 degrees aside from borescope wire direction (Fig. 8).



Fig. 8. Hazet borescope probe [17]

Research has been performed through engine features enabling inspection. The entrance areas are depicted in Fig. 9. The following borescope entrances were used:

- (1) – Spark igniter aperture (after removing the igniter). The inspection included combustion chamber, swirler, fuel injector, high pressures turbine nozzles and blades.
- (2) – Engine inlet. It allowed compressor blades and vanes inspection.
- (3) – Engine outlet. It let access to the power turbine shrouded blades and vanes.
- (4) – EGT thermocouple aperture.
- (5) – Compressor discharge port for centrifugal compressor rotor.

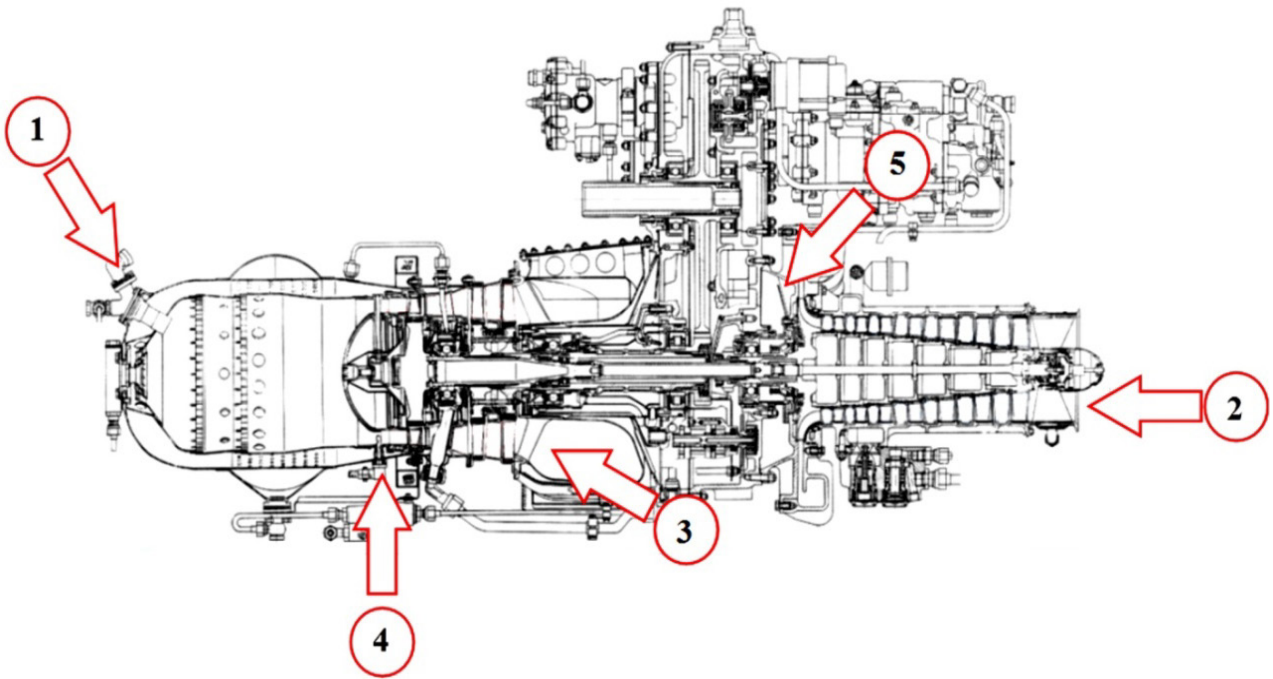


Fig. 9. GTD-350 cross-section with borescope entrances (1-5) [18]

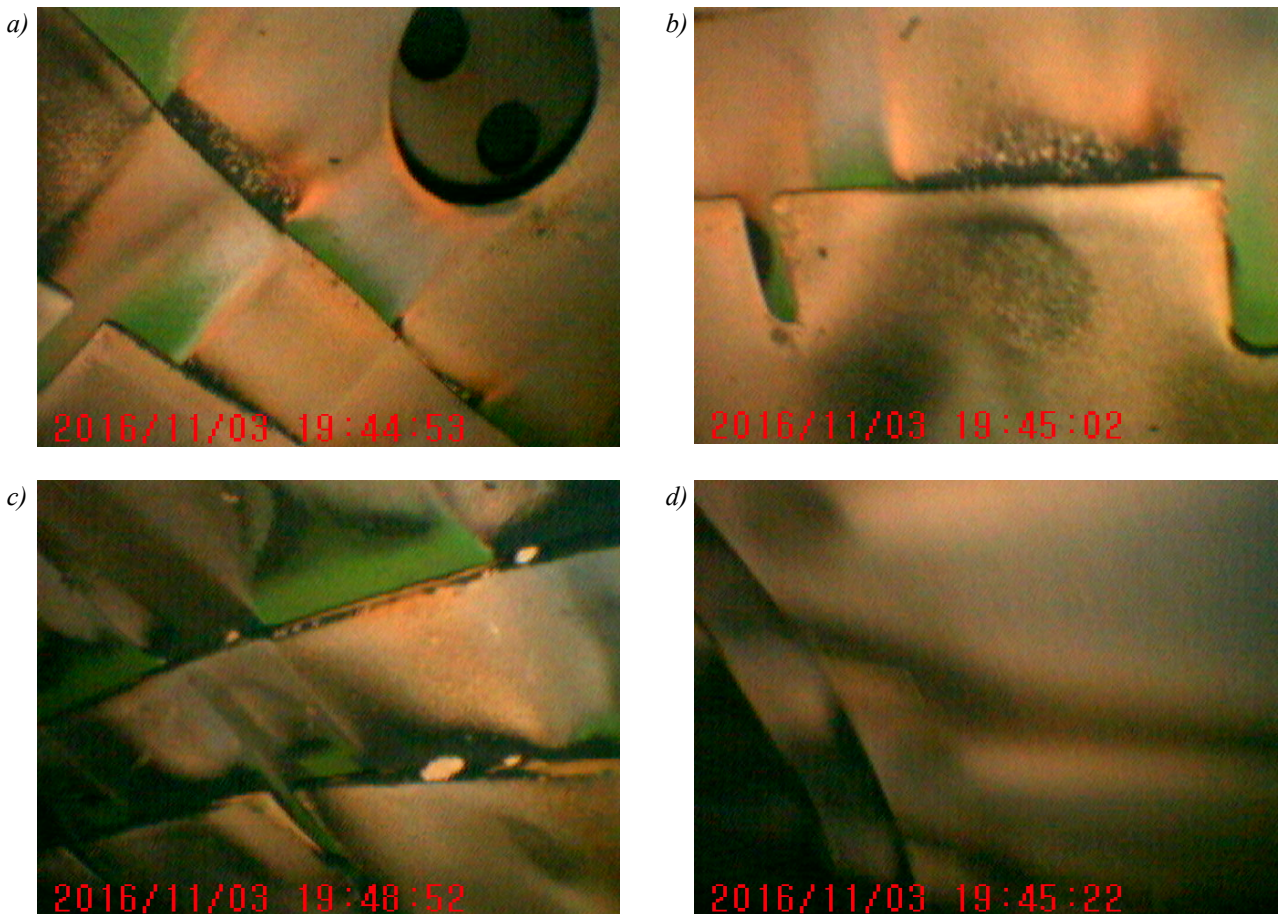


Fig. 10. GTD-350 combustion chamber liners

Results of the combustion chamber borescope inspection are documented in Fig. 10. Combustor liners with dilution and cooling holes are clearly visible. There are no visible cracks or burn through areas, though. The apertures are neither deformed nor overstressed. There is however

sign of coking, fuel deposit and material discoloration. The remaining of the original anti-oxidation green paint is visible in the photos.

Figure 11 shows the fuel injector. High amount of carbon accumulation and coking can be recognized on the deflector surface. The coking, as seen in Fig. 11, is not regarded dangerous, nevertheless it reduces combustion chamber heat exchange coefficient. Reduction of heat exchange rate results in less efficient deflector cooling on the combustor forward wall.

Figure 12 points high-pressure (compressor) turbine nozzles. There are no visible cracks, pits nor dents. The leading edge is uniform and smooth. Picture 12d shows EGT thermocouple. The turbine nozzle is the most sensitive and, in the same time, the most limiting element of turbine engine. High temperature combustion gases might easily affect its structure leading to significant deterioration. In case of given GTD-350 engine, the well-planned tests and high derate applied during engine run, preserved the nozzle in a good shape.

Figure 13 presents high-pressure (compressor) turbine blades. Again, there is no sign of unwanted findings related to over-temperature or FOD/DOD. There are however several discolorations seen in pictures 13c-13d.

Figure 14a-b shows compressor inlet, Fig. 14c-d shows second stage compressor blades and Fig. 14e-f shows power turbine blades. Remarkable deposit can be observed only in Fig. 14a-b. The build-up affects leading edge, thus reducing compressor efficiency, which can be recognized after close analysis of test data. Additionally, one can see blocked anti-icing system holes, which may results in dangerous after-effects, as, happened on 4th December 2003 in Polish Government Mi-8 helicopter crash where icing was responsible for the engine failure. There are no signs of rubbing between the compressor blades and outer casing. This leads to conclusion that compressor did not exhibit increased vibration nor high manoeuvre loads.

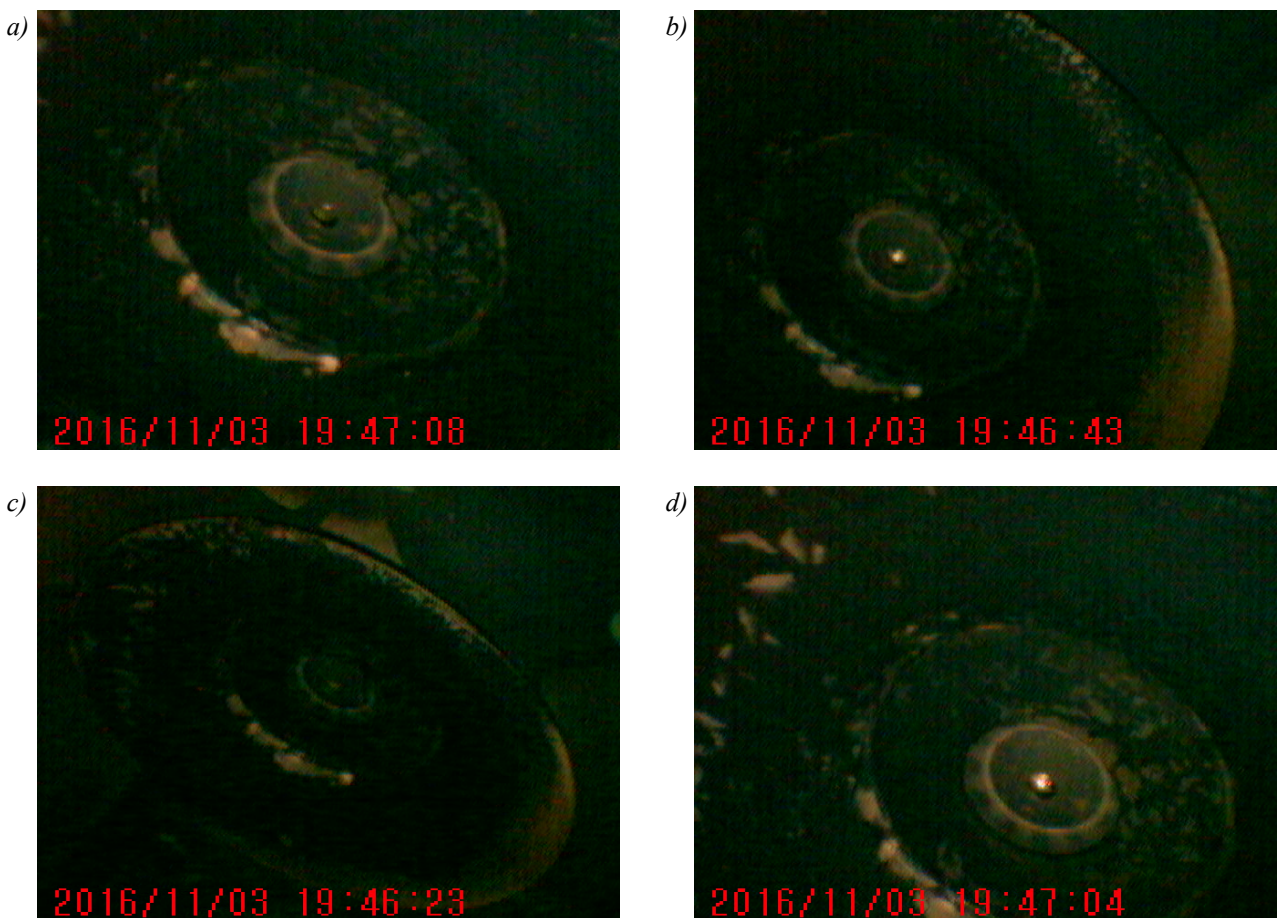


Fig. 11. GTD-350 fuel injector and primary air swirler

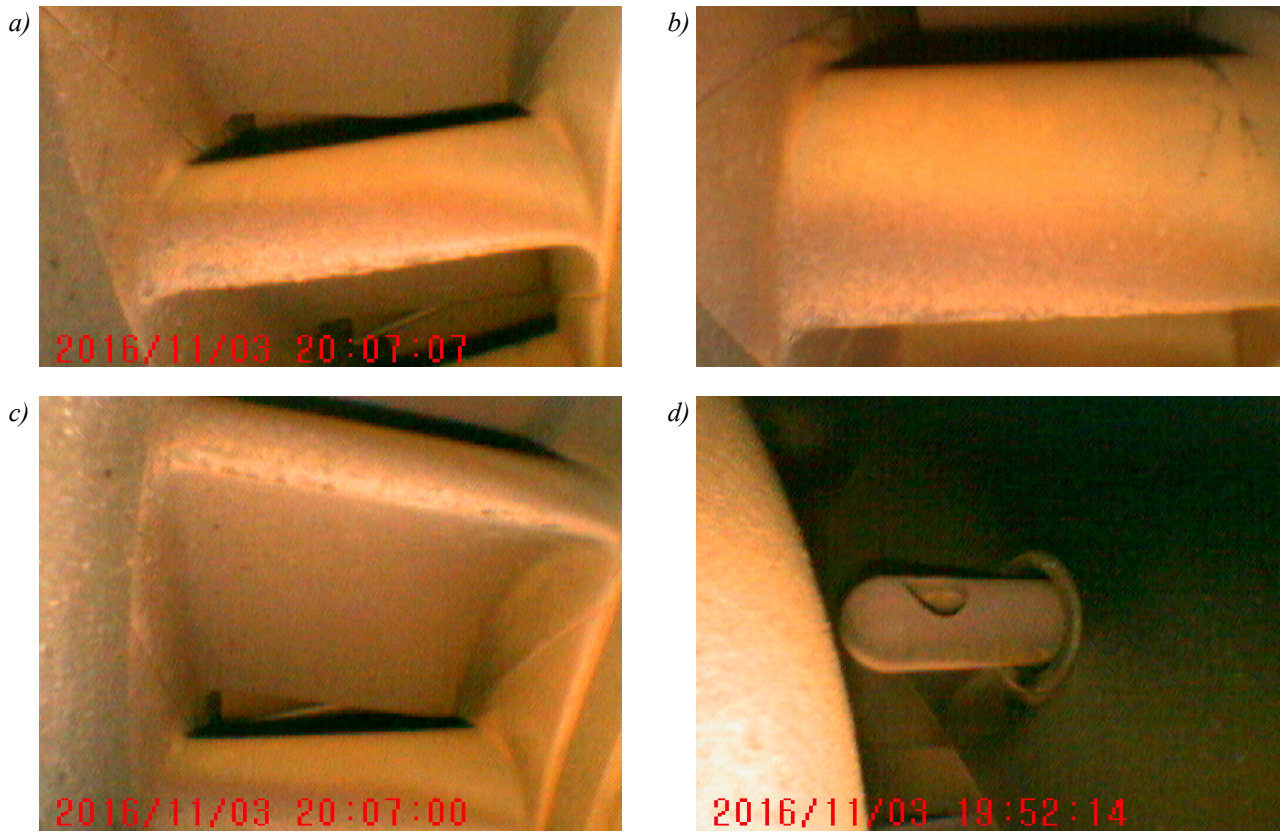


Fig. 12. GTD-350 high-pressure turbine nozzle

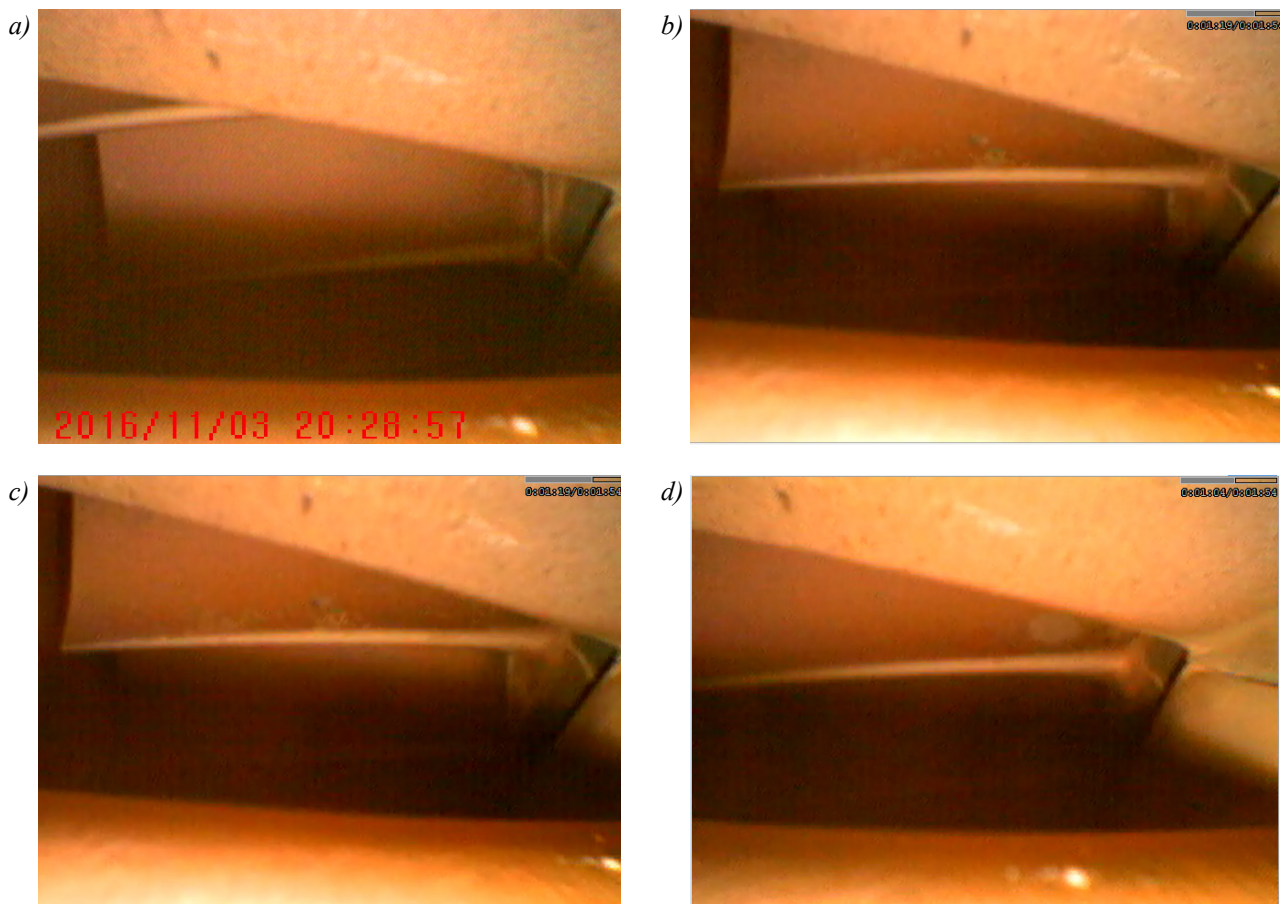


Fig. 13. GTD-350 high-pressure turbine blades



Fig. 14. GTD-350 compressor (a-d) and power turbine blades (e, f)

5. Conclusions

Authors demonstrate advantages of numerical, physics based, CFD modelling in digital analytics predictions of the turboshaft engine deterioration. Due to accurate (but relatively simple at the same time) numerical model it was possible to predict carbon accumulation areas on the forward face of the combustion chamber. Additionally, predictions of the high temperature on the forward side of the primary dilution holes correlated well with borescope observations of the combustor liner deterioration. Carbon accumulation is suspected to be partly caused by a specific engine operation regime: high number of engine starts may be correlated with low operation times. In conclusion, it can be stated that the CFD model can also be used to optimize the geometry of the combustion chamber and the fuel nozzles in the context of improving the quality of the combustion process and minimize harmful emissions.

The overall, observed engine deterioration is well within acceptable limits. There is no significant combustor, nor turbine deterioration apart from compressor build-up. The condition has been predicted based on analysis of registered analytical data. BSI was scheduled and confirmed the findings. Recommended preventive action will include engine cleaning and testing.

High margin of performance and low deterioration is related to applied engine derate. Very often, engine's operating temperature is less than 600°C. Predictive analytics and immediate extensive inspections may keep the engine in use without unexpected events.

Experience connected to digital data is now and for the foreseeable future required for efficiently implement digital engine analytics. Parameters correlation does not easily determine the actual condition of the turbine engine. It also requires reduction to ambient values and high level of system understanding.

Acknowledgments

The scientific work presented in this article was possible thank to the the European Funds, Innovative Economy Programmed 2007-2014 project POIG.02.02.00-14-022/09-00. Modernization and construction of new infrastructure and scientific research for the Military University of Technology and Warsaw University of Technology for joint numerical and experimental studies of turbine engines: Task No. 5 "Modernization of the test benches for the combustion chambers" and Task No. 6 "Modernization of the GTD-350 helicopter engine test bench".

References

- [1] Herbert, L., *Designing for Reliability, Maintainability, and Sustainability (RM&S) in Military Jet Fighter Aircraft Engines*, Master Thesis, Massachusetts Institute of Technology, 2002.
- [2] Kumar, U. D., Crocker, J., Knezevic, J., *Evolutionary Maintenance for Aircraft Engines*, Proceedings Annual Reliability and Maintainability Symposium, pp. 62-68, 1999.
- [3] Batalha, E., *Aircraft Engines Maintenance Costs and Reliability. An Appraisal of the Decision Process to Remove an Engine for a Shop Visit Aiming at Minimum Maintenance Unit Cost*, Master Thesis, Universidade Nova de Lisboa, 2012.
- [4] Kozik, P., Sep, J., *Aircraft Engine overhaul demand frecasting unsin ANN*, Management and Production Engineering Review, Vol. 3, No. 2, pp. 21-26, 2012.
- [5] Liu, D., Zhang, H., Polycarpou, M., Alippi, C., He, H., *Elman-Style Process Neural Network with Application to Aircraft Engine Health Condition Monitoring*, Advances in Neural Networks, Proceedings of the 8th International Symposium on Neural Networks, Guilin, China 2011.
- [6] Soumitra, P., Kapoor, K., Jasani, D., Dudhwewala, R., Gowda, V. B., Gopalakrishnan Nair T.R., *Application of Artificial Neural Networks in Aircraft Maintenance, Repair and Overhaul Solutions*, Analysis and Manufacturing Technologies, 2008.
- [7] Kopytov, E., Labendik, V., Yunusov, S., Tarasov, A., *Managing and Control of Aircraft Power Using Artificial Neural Networks*, Proceeding of the 7th International Conference Reliability and Statistics in Transportation and Communication, 2007
- [8] Garcia Nieto, P. J., Garcia-Gonzales, E., Sanches Lasheras, F., de Cos Juez, F. J., *Hybrid PSO-SVM-based method for forecasting of the remaining useful life for aircraft engines and evaluation of its reliability*, Reliability Engineering & System Safety, Vol. 138, pp. 219-231, 2015.
- [9] Simon, D. L., *An Integrated Architecture for On-Board Aircraft Engine Performance Trend Monitoring and Gas Path Fault Diagnostics*, 57th Joint Army-Navy-NASA-Air Force (JANNAF) Propulsion Meeting sponsored by the JANNAF Interagency Propulsion Committee, 2010.

- [10] Krajček, K., Nikolić, D., Domitrović, A., *Aircraft Performance Monitoring from Flight Data*, Tehnički vjesnik, Vol. 22, No. 5, pp. 1337-1344, 2015.
- [11] Grzegorzewski, J., *Śmigłowiec Mi-2*, Typy broni i uzbrojenia, No. 60, Wydawnictwo Ministerstwa Obrony Narodowej, Warsaw 1979.
- [12] Lubińska, K., *Modernization of the GTD-350 helicopter engine test bench*, ODIUT Automex Sp. z o.o., Gdańsk 2014
- [13] Gieras, M., *Computational study of an aerodynamic flow through a turbine engine combustor*, Archivum Combustionis, Vol. 33, No. 1, pp. 27-40, 2013.
- [14] Gieras, M., *Computational study of a combustion process in a turbine engine combustor*, Archivum Combustionis, Vol. 33, No. 1, pp. 11-26, 2013.
- [15] Gieras, M., *Computational study of the impact of chosen geometry parameters on stability of recirculation zone in GTD-350 gas turbine combustor*, Archivum Combustionis, Vol. 34, No. 2, pp.101-110, 2014.
- [16] ANSYS Inc., ANSYS FLUENT Theory Guide, Release 12.0, 2009.
- [17] <http://hazet.toolteam.de.com/en-GB/hazet-flexible-probe-6mm-4812n-1as-4000896187072.html>.
- [18] [http://www.pwrze.com/gfx/wsk4/userfiles/wsk/produkcja_rodzima/zal_nr_3_gtd-350_wersja_2 pl.pdf](http://www.pwrze.com/gfx/wsk4/userfiles/wsk/produkcja_rodzima/zal_nr_3_gtd-350_wersja_2_pl.pdf).